



OPEN ACCESS

EDITED BY
Caterina Temporini,
University of Pavia, Italy

REVIEWED BY
Roman Řemínek,
Institute of Analytical Chemistry (ASCR),
Czechia
Chongfeng Xu,
Biogen Idec, United States

*CORRESPONDENCE
Nathan Oien,
✉ noien@shattucklabs.com

RECEIVED 04 November 2025
REVISED 17 February 2026
ACCEPTED 23 February 2026
PUBLISHED 12 March 2026

CITATION
Daniels C, Jones K, Makani V, Schmidt C,
Pate J, Wu D, Schreiber TH, De Silva S,
Shukla A and Oien N (2026) Capillary gel
electrophoresis for the analysis of
heterodimer purity in a highly
glycosylated, bispecific Fc fusion protein.
Front. Anal. Sci. 6:1739382.
doi: 10.3389/frans.2026.1739382

COPYRIGHT
© 2026 Daniels, Jones, Makani, Schmidt,
Pate, Wu, Schreiber, De Silva, Shukla and
Oien. This is an open-access article
distributed under the terms of the [Creative
Commons Attribution License \(CC BY\)](#).
The use, distribution or reproduction in
other forums is permitted, provided the
original author(s) and the copyright
owner(s) are credited and that the original
publication in this journal is cited, in
accordance with accepted academic
practice. No use, distribution or
reproduction is permitted which does not
comply with these terms.

Capillary gel electrophoresis for the analysis of heterodimer purity in a highly glycosylated, bispecific Fc fusion protein

Caroline Daniels¹, Kyle Jones¹, Vishruti Makani¹, Cole Schmidt¹, Joseph Pate¹, Dan Wu¹, Taylor H. Schreiber², Suresh De Silva², Abhinav Shukla¹ and Nathan Oien^{1*}

¹Technical Operations, Shattuck Labs, Durham, NC, United States, ²Research and Development, Shattuck Labs, Durham, NC, United States

Introduction: Bispecific therapeutic fusion proteins require analytical methods capable of detecting and resolving process- and product-related impurities while remaining practical to implement and validate. Such methods are essential for supporting both process development and good manufacturing practice (GMP)-compliant testing.

Methods: A sodium dodecyl sulfate capillary gel electrophoresis (CE-SDS) method was developed to separate structurally similar protein species based on differences in the number of N-linked glycosylation sites. The approach leverages glycosylation-dependent electrophoretic mobility to resolve heterodimeric and related molecular species.

Results: The CE-SDS method effectively separated bispecific protein variants that differed in glycosylation, enabling discrimination between the desired bispecific product and associated impurities. This was confirmed by comparing native and deglycosylated Fc-fusion protein. The method was successfully applied to inform process development decisions aimed at enriching the target bispecific protein and was demonstrated to be suitable for GMP release and stability testing by verifying ICH criteria for method validation.

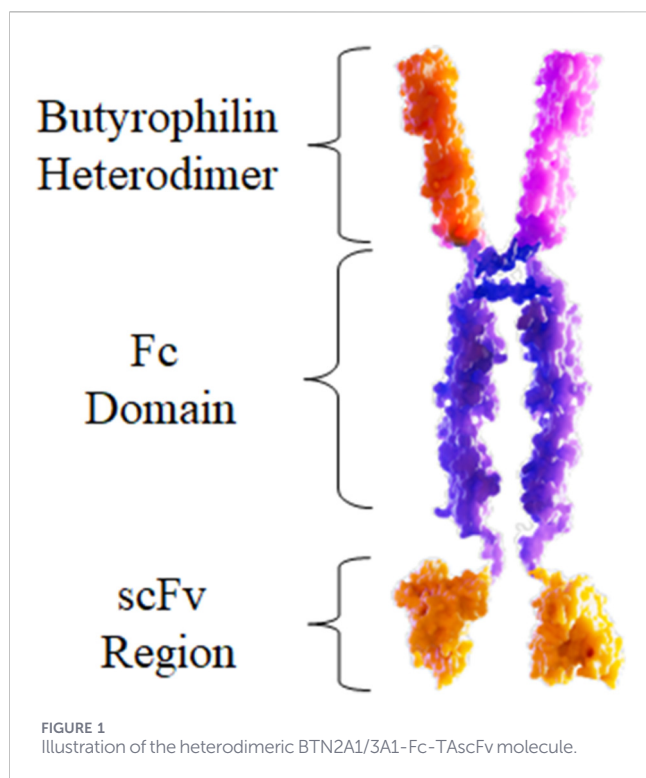
Discussion: This analytical strategy provides a robust and broadly applicable means of separating heterodimeric and bispecific glycoproteins based on glycosylation differences. The method can be readily extended to other fusion proteins, provided sufficient glycosylation asymmetry exists between constituent polypeptide chains, making it a valuable tool for both development and manufacturing control.

KEYWORDS

analytical separation, bispecific, capillary electrophoresis, Fc-fusion protein, heterodimer, quality control methods

1 Introduction

Heterodimeric therapeutic proteins provide a mechanism to target multiple disease pathways with a single molecule or a single pathway that requires two distinct proteins for activation (Ha et al., 2016). However, the development and manufacture of heterodimeric proteins have been hindered by the lack of rapid and readily available analytical methods to distinguish homodimer impurities from the target heterodimeric, therapeutic molecule.



These multispecific biotherapeutics are a class of protein-based therapeutics with the potential to provide significant benefit to patients in areas of unmet medical need. The ability to possess multiple functions or targets in the same molecule provides unique biological and clinical benefits. Bispecific protein therapeutics dominate the multispecific landscape and can be IgG-like or non-IgG-like (Ma et al., 2021). The most common form of bispecifics are antibodies (BsAbs), which the field has primarily leveraged as T-Cell engagers (Wu et al., 2021). Many other forms of bispecific therapeutics exist (including DARTs, BiTes, Nanobodies etc.) and offer significant clinical promise. Fc-Fusion proteins are another class of heterodimeric therapeutic proteins that include cytokines promising for cancer immunotherapy (Möller et al., 2025). A significant area of focus has been the design of better molecules that promote heterodimerization between the two Fc containing halves of the molecule (Wang et al., 2019). Without promotion of heterodimerization, >90% of the products formed could be mispaired if pairing occurs randomly (Chen and Zhang, 2021). Both steric fit and electrostatic interactions have been exploited to promote heterodimerization. The knobs-into-holes approach relies on a steric fit between two different Fc regions that also makes homodimer formation unfavorable (Xu et al., 2015; Duivelshof et al., 2022). An alternative approach has been to employ electrostatic effects to encourage heterodimeric pairing (Gunasekaran et al., 2010). Specifically, for BsAbs, another approach has been to utilize the same heavy chain, but have a kappa and a lambda light chain on each half of the molecule, known as a $\kappa\lambda$ body (Fischer et al., 2015). This approach relies on the use of downstream purification techniques with affinity for the kappa or lambda light chains to generate a pure heterodimer. Yet another approach has been to engineer the Fc binding region such

that one of the heavy chains does not bind to Protein A (Tustian et al., 2016). This enables isolation of the heterodimer during the capture chromatography step itself. However, the characterization of BsAbs and related bispecifics has been obscured by the degree of similarity between the two-halves of the molecule (Sharkey et al., 2017; Karbyshev et al., 2025). The detection and quantification of impurities is essential to the manufacture of therapeutic proteins. Cell culture and downstream purification processes can only be developed and optimized with the use of a quantitative analytical method to separate the desired heterodimeric form from the undesired homodimeric species. Heterodimeric proteins, including BsAbs, present a unique challenge to process development in that they are often structurally similar to the homodimer impurities generated during the upstream process (Dillon et al., 2017).

The two-halves of a bispecific molecule are often nearly identical in size, isoelectric point, and hydrophobicity leaving little opportunity for a high-throughput, quantitative analytical method to be implemented early in process development (Tustian et al., 2016; Sharkey et al., 2017; Dillon et al., 2017; Cao et al., 2018). If the two proteins are sufficiently different in any of the previously mentioned categories, size exclusion chromatography (SEC), charge based methods, and/or hydrophobic interaction chromatography have respectively been utilized to provide resolving power for purity analysis (Cao et al., 2018; Woods et al., 2013; Wang et al., 2018; Grunert et al., 2022; Fekete et al., 2016). Alternate analytical techniques are required when these properties are not sufficiently different between the homodimeric and heterodimeric species. Homodimers are considered inactive impurities and can pose a safety risk. Like other process related impurities, they must be cleared to an appropriate level.

A novel, heterodimeric, bispecific Fc fusion protein has been created to activate $\gamma\delta$ T lymphocytes and promote targeted killing of tumor cells. Each polypeptide chain consists of an extracellular domain of a specific butyrophilin protein (BTN2A1 or BTN3A1) on one end, which is linked via an Fc domain, to a tumor antigen (TA)-specific single-chain antibody fragment (scFv) on the opposing end (Figure 1). The two chains dimerize to form a bispecific heterodimer (termed BTN2A1/3A1-Fc-TAscFv) that directs Vg9Vd2 T cell receptor expressing human T cells to kill tumor cells expressing the tumor antigen targeted by the scFv domain (Lai et al., 2022). Each half of the bispecific fusion protein produced is the same single cell line. As a result the upstream (cell culture) biomanufacturing process is expected to produce BTN2A1 and BTN3A1 homodimer impurities in addition to the therapeutic BTN2A1/3A1 heterodimer. As shown in Table 1, the BTN2A1 and BTN3A1 homodimers as well as the BTN2A1/3A1 heterodimer all have slight differences in molecular weight and charge that could be used for separation. However, the molecular weights of each structure are very close to each other and the use of charge-based separations is further complicated by extensive posttranslational modifications, which includes glycosylation. A notable difference between the BTN2A1 and BTN3A1 polypeptide chains is the extent of glycosylation in the BTN domains. Based on the polypeptide chain sequences, the BTN2A1 chain is expected to contain 7 N-linked glycosylation sites with the BTN3A1 chain expected to contain 3. Therefore, the BTN2A1/3A1 heterodimer is expected to contain ten N-linked

TABLE 1 Predicted Characteristics of BTN2A1/3A1 homo and heterodimers.

Structure	Predicted size	Predicted pI	Predicted number of N-Glycan sites
BTN2A1 homodimer	155.4	8.4	14
BTN3A1 homodimer	154.9	7.4	6
BTN2A1/3A1 heterodimer	155.1	7.7	10

glycosylation sites with the BTN2A1 and BTN3A1 homodimers containing 14 and 6 sites, respectively. The glycosylation site difference between the BTN2A1 and BTN3A1 polypeptide chains is contributed to differential migration by reduced SDS-PAGE in Lai et al. (2022).

Sodium dodecyl sulfate capillary gel electrophoresis (CE-SDS) (also called capillary electrophoresis-SDS (CE-SDS)) is often used as a more readily quantifiable alternative to SDS-PAGE to characterize low and high molecular weight species (Scheller et al., 2021; Wagner et al., 2020). As such, this platform enables development and optimization of the downstream process for large-scale production of proteins (Scheller et al., 2021; Wagner et al., 2020; Rustandi et al., 2008; Cao et al., 2021; Rouby et al., 2020; Gaza-Bulsecu and Liu, 2008; Lu et al., 2013). Protein analysis by CE-SDS relies on the separation of SDS-labelled protein variants through a sieving matrix in a constant electric field (Scheller et al., 2021; Wagner et al., 2020; Wiesner et al., 2021). During preparation, samples are heat denatured in a buffer matrix containing SDS, which imparts a negative charge on proteins proportional to their molecular size. Although molecular weight is the primary mechanism for separation by CE-SDS, level of glycosylation has been shown to have a significant impact on the observed migration time of glycoproteins (Scheller et al., 2021; Wiesner et al., 2021; Wang et al., 2020). Wang et al. report that one N-linked glycosylation site can increase a glycoprotein's observed molecular weight by up to 10 kDa. Thereby, three proteins nearly identical in molecular weight, but varying in level of glycosylation, would have different migration times by CE-SDS. Degree of glycosylation has also been shown to impact protein separation by SDS-polyacrylamide gel electrophoresis (SDS-PAGE), similar to CE-SDS, which can be used in tandem with Western blot to confirm the identity of a species (Scheller et al., 2021; Wang et al., 2020).

Here we present a new method for purity determination of heterodimer content using sodium dodecyl sulfate capillary gel electrophoresis (CE-SDS) for a fusion protein where the homodimers are closely related to the heterodimer product. This analytical method enables accurate and rapid quantification of heterodimer purity making it an ideal method to support process development efforts, as well as test drug substance product purity during batch release and stability testing in quality control.

2 Materials and methods

2.1 Protein expression and purification

For initial development, BTN2A1 and BTN3A1 homodimers as well as the BTN2A1/3A1 heterodimer were produced in ExpiCHO-S

cells. ExpiCHO-S cells were transiently transfected with proprietary plasmids created by Shattuck Labs encoding the BTN2A1 chain and/or BTN3A1 chain using polyethylenimine (PEI). Following transfection, cells were cultivated at 37 °C and 5% CO₂ in a humidified atmosphere with constant shaking at 130 RPM for 24 h. Cells were supplemented with appropriate feeding solution and glucose. The culture medium was harvested 9 days after transfection with the secreted recombinant proteins purified using an affinity capture resin.

For stable cell line development, CHO-DG44 cells were transfected with Shattuck proprietary plasmid encoding the BTN2A1 and BTN3A1 chains using electroporation method to produce BTN2A1/3A1 heterodimer. Two days post-transfection, cells were selected using different concentrations of methotrexate (MTX) to generate minipools. After complete recovery under MTX selection, minipools were scaled-up from static stages through shake flask based on growth and titer data. Top minipool was single cell cloned using Solentim VIPS cell sorter. After monoclonality verification, single cell clones were scaled-up through static stages (96-well plate, 24-well plate, and 6-well plates). Top clones at the 6-well plate stage were evaluated for product titer, followed by scale-up of top clones to shake flask. Based on 14-day shake flask fed-batch data, the top clone was selected and used for upstream processing.

The in-process CHO-DG44 material assessed in these experiments was generated using a 3-step chromatography process. The first unit operation consisted of an affinity-based capture chromatography step operated in bind and elute mode. The product pool was subsequently purified using a mixed-mode intermediate chromatography step operated in bind and elute mode. The final unit operation was an ion exchange polishing chromatography step operated in bind and elute mode. Each unit operation was used to further isolate the target product by removal of process and product related impurities.

2.2 Evaluation of the predicted properties of BTN2A1 homodimer, BTN3A1 homodimer, and the BTN2A1/3A1 heterodimer

The three-dimensional structure of each homodimer was generated using Chai-1. The highest ranked structure with the expected structure was then imported into Schrodinger BioLuminate 6.0. Each molecule was then prepared and analyzed for molecular weight, predicted N-glycan sites, and pI.

2.2.1 SEC

SEC was performed with using a Waters XBridge Premier Protein SEC Column (250Å, 2.5 µm, 4.6 × 300 mm) on a Thermo Fisher Scientific Vanquish HPLC. An isocratic gradient

was used with 20 mM Sodium Phosphate, 350 mM NaCl, pH 7.0, 20% Ethanol at a flow rate of 0.25 mL/min for 20 min, a column temperature of 25 °C, and a column load of 8 µg. Proteins were detected at 280 nm. Column was equilibrated for 30 min and samples were bracketed by a mobile phase blank, a gel filtration standard, and a reference sample. The column was flushed and stored in mobile phase.

2.2.2 MALDI

Analysis was performed by CovalX AG using a Bruker Autoflex II MALDI ToF/ToF mass spectrometer equipped with CovalX's HM4 interaction module. Eight 2-fold serial dilutions in phosphate buffer from 1.25 mg/mL to 5 µg/mL were evaluated for samples. Samples were mixed with a sinapinic acid matrix and 1 µL was spotted on the MALDI plate, which after crystallization, was run on the MADLI mass spectrometer. The remaining sample amount was mixed with DSS and DMF and ran on MATLI-TOF MS. Analysis was performed using a nitrogen laser which focused on ranges of 1–1,500 kDa. CovalX's interaction module contains a special detecting system designed to optimize detection up to 2 MDa with nano-molar sensitivity.

2.2.3 icIEF

Samples were prepared by diluting to 0.2 mg/mL in a master mix containing 9 M urea, 2 M N-ethylurea, 0.35% methyl cellulose, 4% 3–10 Pharmalyte™, 1% 4.5 pI marker, 1% 9.5 pI marker, and 5 mM phosphoric acid. For analysis, samples were transferred to a 96-well plate and placed in a ProteinSimple Maurice set at 10 °C with a cIEF cartridge installed. All samples were loaded for 55 secs with separation occurring at 750 V for 1 min, 1100 V for 1 min, 1500 V for 1 min, and 3000 V for 20 min. Fluorescent detection was utilized with a 3 s exposure. Data was collected through Compass software and analyzed through Empower software.

2.2.4 CE-SDS

Samples were diluted to 1 mg/mL in ProteinSimple CE-SDS PLUS 1X Sample Buffer containing a 10 kDa standard with either 12.5 mM iodoacetamide for non-reducing conditions or 5 mM neutralized Tris (2-carboxyethyl) phosphine for reducing conditions. Both reduced and non-reduced samples were heat denatured for 10 min at 60 °C. For analysis, samples were transferred to a 96-well plate and placed in a ProteinSimple Maurice set at 10 °C. Reduced and non-reduced CE-SDS samples were evaluated using both a ProteinSimple CE-SDS PLUS cartridge as well as a ProteinSimple Turbo cartridge. The CE-SDS PLUS cartridge has an effective capillary length of 20 cm. Samples were loaded for 20 s at 4600 V with separation occurring at 5750 V with run times of 40 and 55 min for reduced and non-reduced samples, respectively. The Turbo cartridge has an effective capillary length of 15 cm. Samples were loaded for 8 s at 3500 V with separation occurring at 4200 V with run times of 12 and 14 min for reduced and non-reduced samples, respectively. Data was collected and analyzed through Empower software.

N-linked deglycosylation was performed by heat denaturing samples at 70 °C for 5 min in the presence of 0.8% Rapigest™ SF

(Waters, Catalog # 186008090). Samples were then combined with 6 µL of Rapid™ PNGase F, non-reducing format, (New England BioLabs, Catalog #P0711S) and placed at 50 °C for 10 min. Samples were allowed to cool to room temperature and buffer exchanged into CE-SDS PLUS 1X Sample Buffer to be tested under reduced or non-reduced conditions. The cartridge set up for both reduced and non-reduced CE-SDS was an initial sample load for 20 s at 4,600 volts followed by a voltage of 5,750 for 40 min and 50 min respectively. The cartridge was cleaned using the “cartridge post-cleanup” setting on the ProteinSimple Maurice. The “cartridge post-cleanup” utilizes the wash buffer and water over a 10-min span to clean the cartridge.

2.2.5 SDS-PAGE and western blot

Samples were prepared by diluting to 0.05 mg/mL in NuPAGE™ LDS Sample Buffer with either 12.5 mM iodoacetamide for non-reduced samples or 50 mM dithiothreitol for reduced samples. All samples were heat denatured at 70 °C for 10 min. Proteins were separated on a pre-cast NuPAGE™ 3%–8% Tris-Acetate Gel at 150 V for 60 min. SDS-PAGE gels were coomassie stained and destained with a Genscript eStain device.

For Western blot analysis, proteins separated by SDS-PAGE were transferred to a nitrocellulose membrane and blocked using 1X Tris Buffered Saline (TBS) with 1% Casein. For primary antibody binding the blot was incubated with 0.2 µg/mL sheep anti-human BTN3A1/2/3 antibody and 0.5 µg/mL rabbit anti-human BTN2A1 antibody in 1X TBS 1% Casein, 0.02% Tween 20 for 1 h. Following incubation, the blot was washed with 1X TBS, 0.1% Tween 20. For secondary antibody binding the blot was incubated for 1 h with LI-COR® IRDye® 800CW donkey anti-goat (1:10,000) and BioRad StarBright Blue 520 goat anti-rabbit (1:2,500) antibodies in 1X TBS, 1% Casein, 0.02% Tween 20. SDS-PAGE gels and western blots were imaged using a BioRad ChemiDoc™.

2.2.6 Biolayer interferometry (BLI)

BLI on the Sartorius Octet® HTX platform was performed with Sartorius SA biosensors loaded with biotinylated anti-BTN2A1 camelid antibodies developed in conjunction with Thermo Scientific. Following a 30 s baseline step samples serially diluted 100–0.05 µg/mL were loaded onto biosensors for 120 s. After a 30 s baseline step, mouse anti-BTN3A1/2/3 antibody (R&D Systems, Catalog # MAB7136) at 20 µg/mL was loaded for 200 s. Dose response curves were generated by Softmax Pro.

3 Results

3.1 Evaluation of BTN2A1 and BTN3A1 homodimer by SEC, MALDI and icIEF analytical platforms

BTN2A1 and BTN3A1 homodimeric Fc fusion protein controls produced and purified from transiently transfected mammalian cells were analyzed by SEC. After including theoretical post translational modifications, BTN2A1 and BTN3A1 homodimers differed in molecular weight by approximately 15 kDa. The SEC profiles in **Figure 2** demonstrate a difference in retention time for the

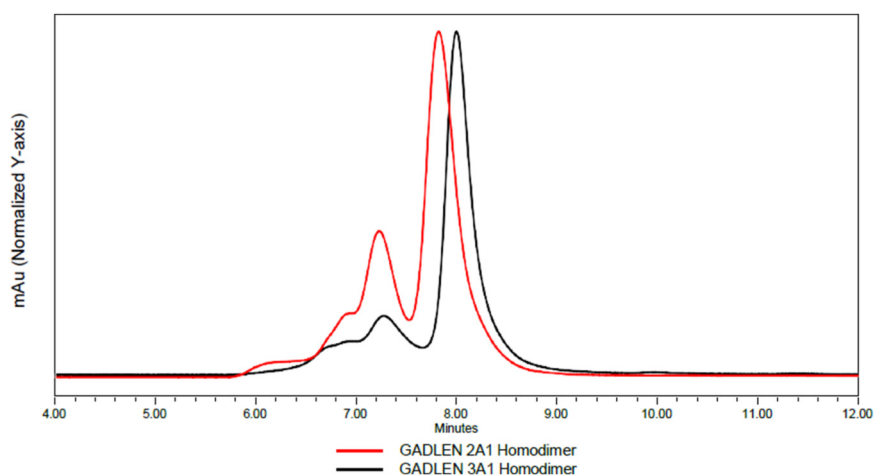


FIGURE 2
BTN2A1 and BTN3A1 homodimer controls analysis by SEC.

homodimers at approximately 8 min, however, the theoretical USP resolution between the two peaks was 0.34, which is not sufficient to provide a quantitative assessment of purity.

Matrix Assisted Laser Desorption/Ionization (MALDI) mass spectrometry analysis was also performed with the BTN2A1 and BTN3A1 homodimers to determine their molecular weight (Figure 3). Observed molecular weights for the BTN2A1 and BTN3A1 homodimers were determined to be 175.7 and 160.8 kDa, respectively, confirming the larger molecular weight of the BTN2A1 homodimer due to post-translational modifications. A second prominent peak was observed in the BTN3A1 homodimer sample at approximately 110 kDa. Based on the molecular weight, this peak was identified to be the dimer species missing both BTN3A1 domains. This species was determined to be a method artifact as the impurity was not observed in an orthogonal assay (e.g., non-reducing CGE). Although MALDI was able to show a molecular weight difference between the two homodimers, the non-quantitative nature of the platform would not make it suitable for analyzing process development samples with a high degree of heterogeneity. Furthermore, the molecular weight difference between the homodimers and heterodimer would not allow for sufficient resolution in a heterogeneous sample.

BTN2A1 and BTN3A1 homodimers were evaluated by imaged capillary isoelectric focusing (icIEF) for apparent charge difference. The BTN2A1 homodimer profile contains multiple peaks with isoelectric points ranging from 7.4–8.1 (Figure 4). In contrast, the BTN3A1 homodimer profile contains a main peak with an apparent pI of 7.7. Overlap in the apparent isoelectric points of the BTN2A1 and BTN3A1 chains prevented the use of other charge-based methods for separation.

3.2 Evaluation of BTN homodimers and BTN2A1/3A1 heterodimer by CE-SDS

For this evaluation a BTN2A1/3A1 heterodimer produced similarly to the homodimers was evaluated by CE-SDS. Peak

relative migration time (RMT) was calculated based on the migration time as compared to a 10 kDa standard. Under reducing conditions, RMTs of 1.85 and 2.04 were observed for the BTN3A1 and BTN2A1 homodimer controls, respectively (Figure 5). Two prominent peaks were observed in the reduced BTN2A1/3A1 heterodimer sample at 1.85 and 2.03 aligning with the BTN2A1 and BTN3A1 monomers. These peaks will be referred to as Peak 1-R and Peak 2-R in the order of their increasing RMT. RMTs of 2.35 and 2.62 were observed for the non-reduced BTN3A1 and BTN2A1 homodimer controls, respectively (Figure 6). Likewise, prominent peaks were observed in the BTN2A1/3A1 heterodimer sample at RMTs of 2.37 and 2.60. Notably, a peak was also present in the sample at a RMT of 2.48. These peaks will be referred to as Peak 1-NR, Peak 2-NR, and Peak 3-NR in the order of their increasing RMT.

To determine if degree of glycosylation was the primary mechanism for peak separation, samples were digested with PNGase F to remove N-linked glycans. Samples were subsequently evaluated by reduced and non-reduced CE-SDS. Under reducing conditions, a single peak is observed in all three samples at a RMT of 1.7 (Figure 7). Under non-reducing conditions, the BTN2A1 and BTN3A1 homodimer controls as well as the BTN2A1/3A1 heterodimer sample all contain a single peak with a RMT of 2.2 (Figure 8).

3.3 Evaluation of BTN homodimers and BTN2A1/3A1 heterodimer by SDS-PAGE and Western blot

To verify whether the peaks observed in the CE-SDS profile correspond to the respective BTN chains, the BTN2A1 and BTN3A1 homodimers were analyzed by SDS-PAGE and Western blot alongside the BTN2A1/3A1 heterodimer. Under reduced SDS-PAGE conditions bands are present at approximately 84 and 76 kDa for the BTN2A1 and BTN3A1 monomers, respectively, corroborating the increased observed molecular weight of the

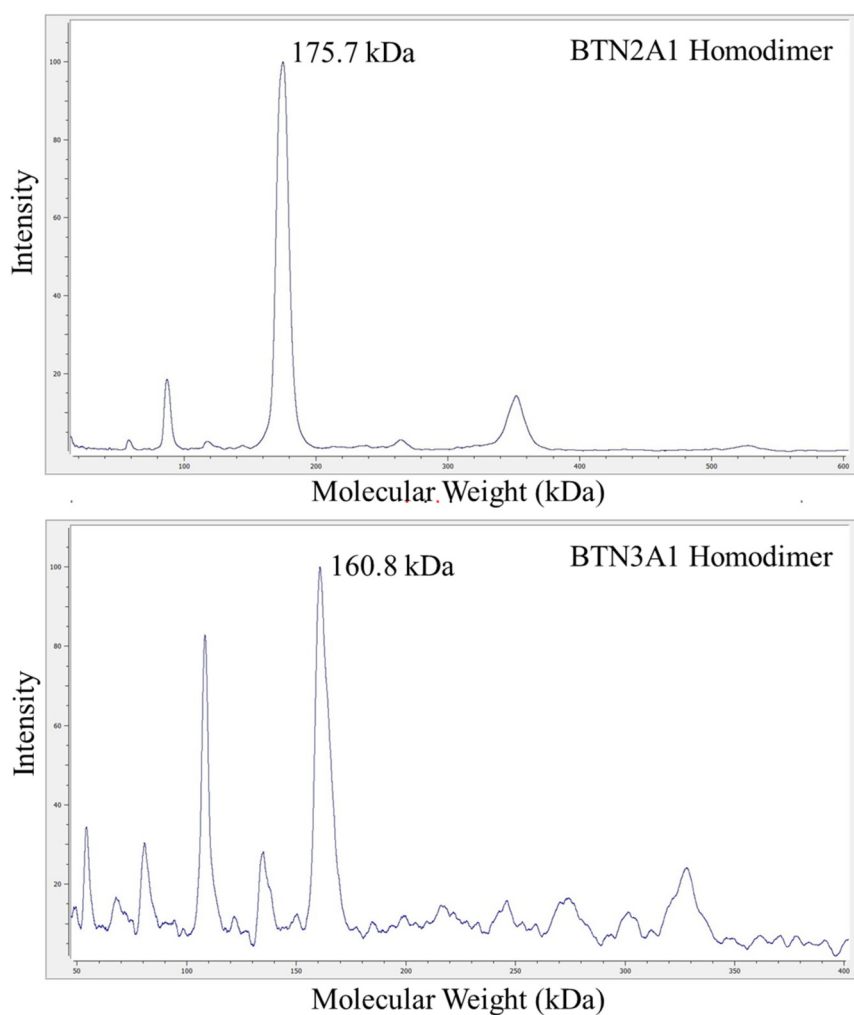


FIGURE 3
BTN2A1 and BTN3A1 homodimer controls analysis by MALDI mass spectrometry.

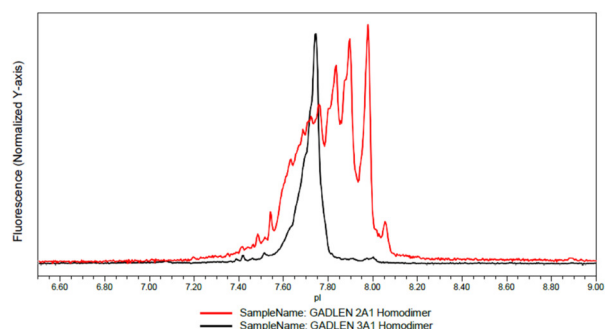


FIGURE 4
BTN2A1 and BTN3A1 homodimer controls analysis by (c) icIEF.

BTN2A1 homodimer (Figure 9, lanes 5 and 6). Comparable to CE-SDS, two bands are present in the reduced BTN2A1/3A1 heterodimer sample at approximately 83 and 76 kDa (Figure 9, lane 7). When evaluated by non-reduced SDS-PAGE

bands are present at approximately 192 and 181 kDa for the BTN2A1 and BTN3A1 homodimer controls, respectively (Figure 9, lanes 2 and 3). Similar to CE-SDS, three bands are present in the BTN2A1/3A1 heterodimer sample at approximately 193, 186, and 181 kDa suggestive of the presence of the two homodimers and a heterodimeric species (Figure 9, lane 4).

Western blot analysis was performed with a SDS-PAGE gel using antibodies specific to the BTN2A1 and BTN3A1 domains with corresponding secondary detection antibodies conjugated with IR-dyes. Bands containing the BTN2A1 domain were pseudo-colored in blue with bands containing the BTN3A1 domain pseudo-colored in green. A teal color is produced during detection when there is an overlap of the two pseudo-colors in a specific band. Under reducing conditions, a blue band is observed at 84 kDa in the BTN2A1 homodimer control indicating presence of the domain (Figure 10, lane 6). Conversely, a green band is observed at 76 kDa in the BTN3A1 control indicating binding of the BTN3A1 antibody (Figure 10, lane 5). In the BTN2A1/3A1 heterodimer sample the band at 83 kDa is labelled with the BTN2A1 antibody and the band

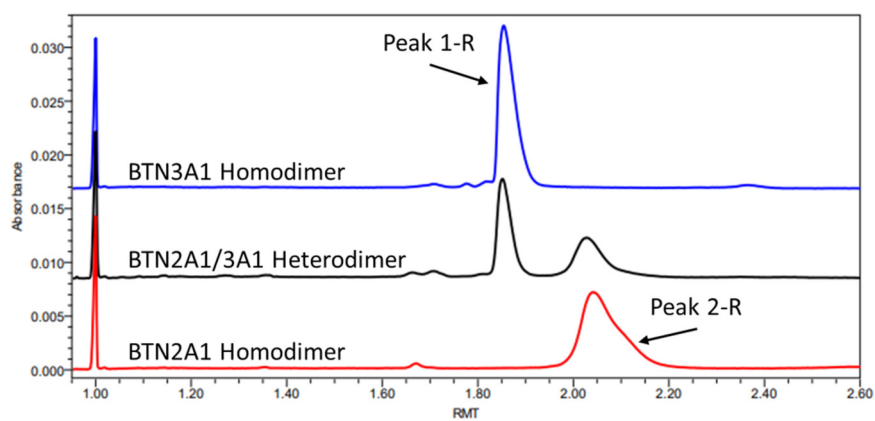


FIGURE 5
CE-SDS analysis of BTN2A1/3A1 heterodimer with BTN2A1 and BTN3A1 homodimer controls under reduced conditions.

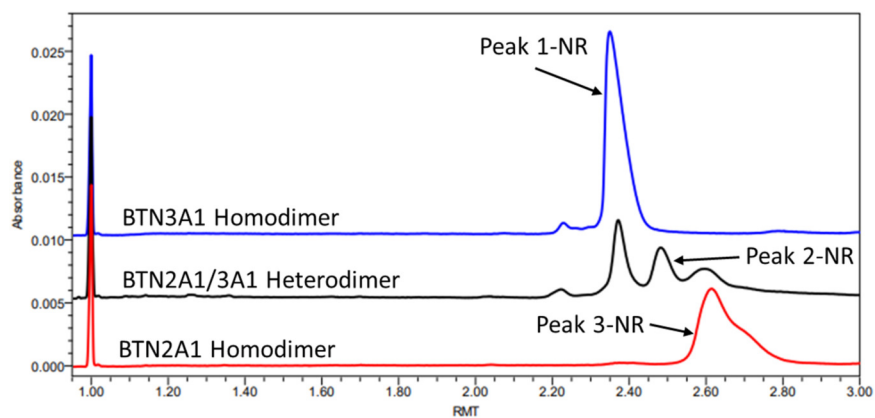


FIGURE 6
CE-SDS analysis of BTN2A1/3A1 heterodimer with BTN2A1 and BTN3A1 homodimer controls under non-reduced conditions.

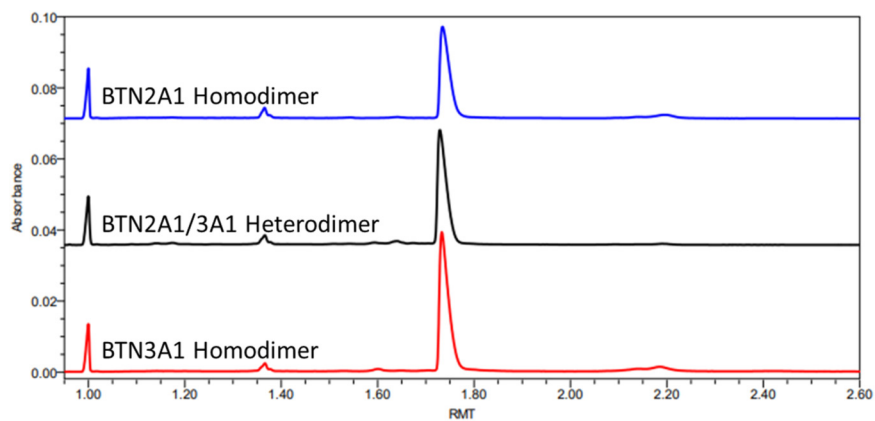


FIGURE 7
Samples were evaluated again following N-linked deglycosylation under reduced conditions.

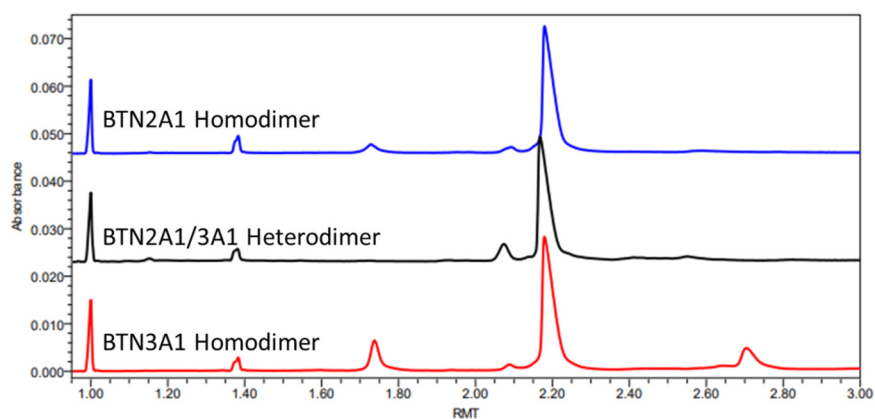


FIGURE 8
Samples were evaluated again following N-linked non-reduced conditions.

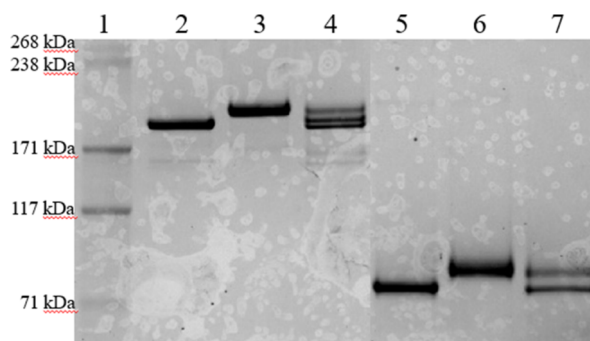


FIGURE 9
SDS-PAGE of BTN2A1/3A1 heterodimer with BTN2A1 and BTN3A1 homodimer controls under reduced/non-reduced conditions. (lane 1: protein molecular weight ladder; lane 2: BTN3A1 homodimer, non-reduced; lane 3: BTN 2A1 homodimer, non-reduced; lane 4: BTN2A1/3A1 heterodimer, non-reduced; lane 5: BTN3A1 homodimer, reduced; lane 6: BTN 2A1 homodimer, reduced; lane 7: BTN2A1/3A1 heterodimer, reduced).

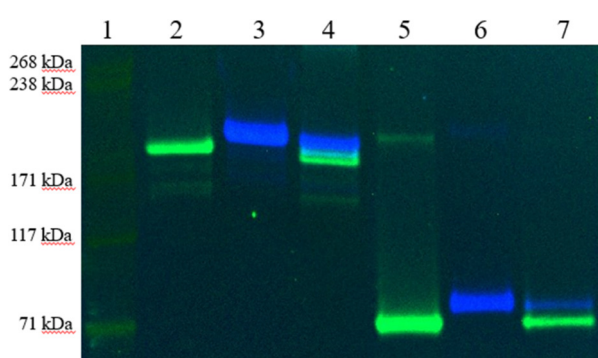


FIGURE 10
Western blot analysis of BTN2A1/3A1 heterodimer with BTN2A1 and BTN3A1 homodimer controls under reduced/non-reduced conditions. (lane 1: protein molecular weight ladder; lane 2: BTN3A1 homodimer, non-reduced; lane 3: BTN 2A1 homodimer, non-reduced; lane 4: BTN2A1/3A1 heterodimer, non-reduced; lane 5: BTN3A1 homodimer, reduced; lane 6: BTN 2A1 homodimer, reduced; lane 7: BTN2A1/3A1 heterodimer, reduced).

at 76 kDa is labelled with the BTN3A1 antibody (Figure 10, lane 7). When evaluating the non-reduced lanes, the BTN2A1 homodimer control at 192 kDa is labelled with the BTN3A1 control at 181 kDa labelled with the BTN3A1 antibody (Figure 10, lanes 2 and 3). The three primary bands observed in the BTN2A1/3A1 heterodimer sample at approximately 193, 186, and 181 kDa were observed to be blue, teal, and green, respectively, indicating the presence of all 3 dimeric species in the purified product (Figure 10, lane 4).

3.4 Enrichment of BTN2A1/3A1 heterodimer and confirmation by BLI

A dual-binding bio-layer interferometry (BLI) assay utilizing antibodies specific to the BTN2A1 and BTN3A1 butyrophilins was adopted to evaluate downstream process intermediates for heterodimer enrichment. During scale-up a CHO-DG44 clone was selected for heterodimer production. Chromatography eluates were compared after capture and following a polishing step designed to enrich for Peak 2-NR in the CE-SDS profile. By

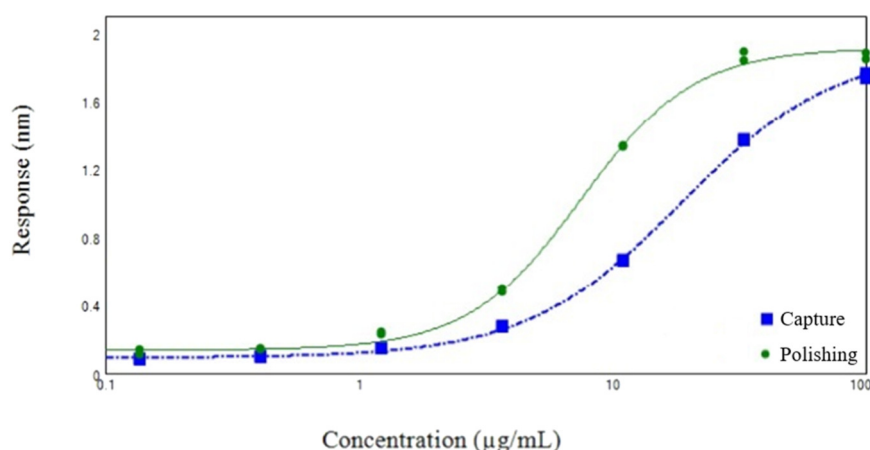


FIGURE 11
Dose response curves generated using a dual binding BLI method to compare downstream process intermediates.

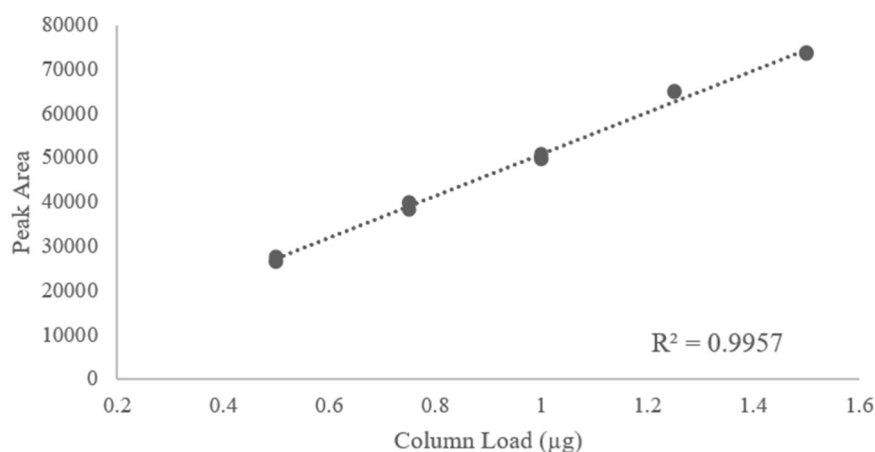


FIGURE 12
Linearity assessment of CE-SDS for the analysis of BTN2A1/3A1 heterodimer.

non-reduced CE-SDS Peak 2-NR content increase from 24.6% post-capture to 76.7% after polishing (data not shown). Comparing the dose response curves generated by BLI, EC₅₀ was calculated to be 18.6 µg/mL at capture and decreased to 7.5 µg/mL following polishing (Figure 11).

3.5 Method validation

The CE-SDS method was validated by assessing linearity, repeatability, and accuracy for the BTN2A1/3A1 heterodimer and both BTN2A1 and BTN3A1 homodimer peaks across a range of concentrations. A single sample was diluted to 0.5, 0.75, 1.0, 1.25, and 1.5 mg/mL with each concentration prepared in triplicate. The coefficient of determination (R^2) for the BTN2A1/3A1 heterodimer species was 1.00 (Figure 12), while the BTN2A1 and BTN3A1 homodimers yielded R^2 values of 0.99 and 0.98, respectively. Repeatability, evaluated as the %RSD of each triplicate preparation, ranged from 2% to 9% across all concentrations and species (Table 2). Accuracy, assessed through percent recovery, ranged

from 93% to 111% for all species and concentrations (Table 2). The CE-SDS method exhibited strong linearity, precision, and accuracy across the evaluated concentration range, with all parameters meeting typical analytical validation standards. The high correlation coefficients, low %RSD values, and consistent recoveries collectively confirm the method's reliability for quantitative assessment of the BTN2A1/3A1 heterodimer and corresponding homodimers. These findings support the suitability of the CE-SDS method for routine characterization and quality assessment of these species.

4 Discussion

In many cases, post translational modifications complicate the ability to analytically separate impurities that are structurally similar to a target molecule. The post translational modifications often lead to broad peaks that cannot be resolved by size exclusion or charge based methods. Readily available analytical platforms typically require a substantial difference in isoelectric point, molecular

TABLE 2 Reproducibility assessment of CE-SDS for the analysis of BTN2A1/3A1 heterodimer.

Target concentration (mg/mL)	%RSD	%Recovery for triplicate preparations
0.50	2	99
0.75	2	101
1.00	1	99
1.25	0	104
1.50	0	99

weight, or hydrophobicity for robust peak resolution. Methods such as SEC, MALDI, DLS (data not shown), SDS-PAGE, icIEF, and BLI have all been evaluated for relative quantitation of the BTN2A1/3A1 heterodimer species. However, each method lacked sufficient resolution or corresponding quantitative capability. We were able to leverage the number of glycosylation sites as a post translational modification that provides high resolution separation of structurally related species. Based on the peptide sequences of the BTN2A and BTN3A1 chains, four expected N-linked glycosylation sites distinguish the heterodimeric molecule from the BTN2A1 and BTN3A1 homodimers. Peptide map analysis was performed with purified BTN2A1/3A1 heterodimer and confirmed that all theoretical sites were glycosylated (data not shown). Based on the reported CE-SDS results for other glycoproteins each glycosylation site can increase the apparent molecular weight of proteins by up to 10 kDa. As such, a 40 kDa apparent difference can be predicted between the BTN2A1/3A1 heterodimer and the two homodimers. This apparent molecular weight difference was expected to be sufficient for peak separation as the platform is used to detect impurities with a molecular weight difference of ~25 kDa (approximate molecular weight of an antibody light chain).

Reduced CE-SDS with the BTN2A1 and BTN3A1 homodimers revealed baseline resolution between the polypeptide chains even though their theoretical molecular weights are nearly identical. Under non-reducing conditions three prominent peaks were observed in the BTN2A1/3A1 heterodimer sample. Peak 1-NR displayed an identical RMT to the BTN3A1 homodimer with Peak 3-NR aligning with the BTN2A1 homodimer. The BTN2A1/3A1 heterodimer would be expected to migrate between the two homodimers if glycosylation was the primary mechanism for the migration time difference. When deglycosylated all three molecules displayed identical RMTs under both reduced and non-reduced conditions confirming degree of glycosylation is the primary mechanism for peak separation. Glycosylation has also been shown to impact protein separation by SDS-PAGE similar to CE-SDS. Under non-reducing conditions the BTN2A1/3A1 heterodimer sample produced three bands aligning with the CE-SDS profile. A teal color was observed with the band corresponding to Peak 2-NR in the CE-SDS profile indicating the presence of antibodies specific to the BTN2A1 and BTN3A1 domains.

A downstream purification process was developed to enrich for Peak 2-NR in the CE-SDS profile. Chromatography eluates collected after capture and polishing steps were compared by a dual-binding BTN2A1/3A1 BLI assay. Normalizing sensorgrams to the final association step revealed protein bound by the BTN2A1 and BTN3A1 specific antibodies (i.e., BTN2A1/3A1 heterodimer). The

increase in Peak 2-NR purity by CE-SDS was found to have a nearly identical factor of decrease in EC50 from capture to polishing confirming the enrichment of the heterodimer.

The use of CE-SDS for quantitation of heterodimeric BTN2A1/3A1 molecules is presented herein, however, as the method is based on the number of N-linked glycosylation sites, this method could be broadly adopted to other bispecifics and glycoproteins. This method could be applied to bsAbs, but only if the number of glycosylation sites between the two-halves is different. Conceivably, if the two-halves are similar in all other quality attributes, engineering one-half to include additional N-glycan sites could allow for analytical separation by CE-SDS (similar to pI engineering). This mechanism of separation expands the list of characteristics capable of separating proteins beyond size, isoelectric point, or hydrophobicity.

Data availability statement

The raw data supporting the conclusions of this article will be made available by the authors, without undue reservation.

Author contributions

CD: Formal Analysis, Writing – review and editing, Investigation. KJ: Writing – original draft, Investigation, Validation. VM: Writing – review and editing, Investigation. CS: Writing – review and editing. JP: Writing – review and editing, Investigation. DW: Writing – review and editing, Investigation. TS: Supervision, Writing – review and editing. SD: Writing – review and editing, Supervision. AS: Supervision, Writing – review and editing, Project administration. NO: Project administration, Writing – original draft, Conceptualization, Formal Analysis, Investigation, Software, Writing – review and editing.

Funding

The author(s) declared that financial support was not received for this work and/or its publication.

Acknowledgements

The authors would like to thank CovalX AG for their MALDI mass spectrometry sample analysis.

Conflict of interest

Authors CD, KJ, VM, CS, JP, DW, TS, SD, AS, and NO were employed by Shattuck Labs.

Generative AI statement

The author(s) declared that generative AI was not used in the creation of this manuscript.

Any alternative text (alt text) provided alongside figures in this article has been generated by Frontiers with the support of artificial

intelligence and reasonable efforts have been made to ensure accuracy, including review by the authors wherever possible. If you identify any issues, please contact us.

Publisher's note

All claims expressed in this article are solely those of the authors and do not necessarily represent those of their affiliated organizations, or those of the publisher, the editors and the reviewers. Any product that may be evaluated in this article, or claim that may be made by its manufacturer, is not guaranteed or endorsed by the publisher.

References

- Cao, M., Wang, C., Chung, W. K., Motabar, D., Wang, J., Christian, E., et al. (2018). Characterization and analysis of scFv-IgG bispecific antibody size variants. *MAbs* 10 (8), 1236–1247. doi:10.1080/19420862.2018.1505398
- Cao, M., Jiao, Y., Parthemore, C., Korman, S., Ma, J., Hunter, A., et al. (2021). Identification of a CE-SDS shoulder peak as disulfide-linked fragments from common CH2 cleavages in IgGs and IgG-like bispecific antibodies. *MAbs* 13 (1), 1981806. doi:10.1080/19420862.2021.1981806
- Chen, S., and Zhang, W. (2021). Current trends and challenges in the downstream purification of bispecific antibodies. *Antib. Ther.* 4 (2), 73–88. doi:10.1093/abt/tbab007
- Dillon, M., Yin, Y., Zhou, J., McCarty, L., Ellerman, D., Slaga, D., et al. (2017). Efficient production of bispecific IgG of different isotypes and species of origin in single mammalian cells. *MAbs* 9 (2), 213–230. doi:10.1080/19420862.2016.1267089
- Duivelshof, B. L., Beck, A., Guillaume, D., and D'Atri, V. (2022). Bispecific antibody characterization by a combination of intact and site-specific/chain-specific LC/MS techniques. *Talanta* 236, 122836. doi:10.1016/j.talanta.2021.122836
- Fekete, S., Veuthey, J. L., Beck, A., and Guillaume, D. (2016). Hydrophobic interaction chromatography for the characterization of monoclonal antibodies and related products. *J. Pharm. Biomed. Anal.* 130, 3–18. doi:10.1016/j.jpba.2016.04.004
- Fischer, N., Elson, G., Magistrelli, G., Dheilly, E., Fouque, N., Laundon, A., et al. (2015). Exploiting light chains for the scalable generation and platform purification of native human bispecific IgG. *Nat. Communications* 6, 6113. doi:10.1038/ncomms7113
- Gaza-Bulsecu, G., and Liu, H. (2008). Fragmentation of a recombinant monoclonal antibody at various pH. *Pharm. Res.* 25 (8), 1881–1890. doi:10.1007/s11095-008-9606-3
- Grunert, I., Heinrich, K., Ernst, J., Hingar, M., Briguet, A., Leiss, M., et al. (2022). Detailed analytical characterization of a bispecific IgG1 CrossMab antibody of the Knob-into-Hole format applying various stress conditions revealed pronounced stability. *ACS Omega* 7 (4), 3671–3679. doi:10.1021/acsomega.1c06305
- Gunasekaran, K., Pentony, M., Shen, M., Garrett, L., Forte, C., Woodward, A., et al. (2010). Enhancing antibody Fc heterodimer formation through electrostatic steering effects. *J. Biol. Chem.* 285 (25), 19637–19646. doi:10.1074/jbc.M110.117382
- Karbyshev, M. S., Kalashnikova, I. V., Dubrovskaya, V. V., Baskakova, K. O., Kuzmichev, P. K., and Sandig, V. (2025). Trends and challenges in bispecific antibody production. *J. Chromatogr. A* 1744, 465722. doi:10.1016/j.chroma.2025.465722
- Ha, J. H., Kim, J. E., and Kim, Y. S. (2016). Immunoglobulin Fc heterodimer platform technology: from design to applications in therapeutic antibodies and proteins. *Front Immunol.* 7, 394. doi:10.3389/fimmu.2017.01582
- Lai, A. Y., Patel, A., Brewer, F., Evans, K., Johannes, K., González, L. E., et al. (2022). Cutting edge: bispecific $\gamma\delta$ T cell engager containing Heterodimeric BTN2A1 and BTN3A1 promotes targeted activation of V γ 9V δ 2+ T cells in the presence of costimulation by CD28 or NKG2D. *J. Immunol.* 209 (8), 1475–1480. doi:10.4049/jimmunol.2200185
- Lu, C., Liu, D., Liu, H., and Motchnik, P. (2013). Characterization of monoclonal antibody size variants containing extra light chains. *MAbs* 5 (1), 102–113. doi:10.4161/mabs.22965
- Ma, J., Mo, Y., Tang, M., Shen, J., Qi, Y., Zhao, W., et al. (2021). Bispecific antibodies: from research to clinical application. *Front. Immunol.* 12, 626616. doi:10.3389/fimmu.2021.626616
- Möller, A. M., Vettermann, S., Baumann, F., Pütter, M., and Müller, D. (2025). Trifunctional antibody-cytokine fusion protein formats for tumor-targeted combination of IL-15 with IL-7 or IL-21. *Front. Immunol.* 16, 1498697. doi:10.3389/fimmu.2025.1498697
- Rouby, G., Tran, N. T., Leblanc, Y., Taverna, M., and Bihoreau, N. (2020). Investigation of monoclonal antibody dimers in a final formulated drug by separation techniques coupled to native mass spectrometry. *MAbs* 12 (1), e1781743. doi:10.1080/19420862.2020.1781743
- Rustandi, R. R., Washabaugh, M. W., and Wang, Y. (2008). Applications of CE SDS gel in development of biopharmaceutical antibody-based products. *Electrophoresis* 29 (17), 3612–3620. doi:10.1002/elps.200700958
- Scheller, C., Krebs, F., Wiesner, R., Wätzig, H., and Oltmann-Norden, I. (2021). A comparative study of CE-SDS, SDS-PAGE, and simple Western-precision, repeatability, and apparent molecular mass shifts by glycosylation. *Electrophoresis* 42 (14–15), 1521–1531. doi:10.1002/elps.202100068
- Sharkey, B., Pudi, S., Wallace, M. I., Zhong, L., Prinz, B., Baruah, H., et al. (2017). Purification of common light chain IgG-like bispecific antibodies using highly linear pH gradients. *MAbs* 9 (2), 257–268. doi:10.1080/19420862.2016.1267090
- Tustian, A. D., Endicott, C., Adams, B., Mattila, J., and Bak, H. (2016). Development of purification processes for fully human bispecific antibodies based upon modification of protein A binding avidity. *MAbs* 8 (4), 828–838. doi:10.1080/19420862.2016.1160192
- Wagner, E., Colas, O., Chenu, S., Goyon, A., Murisier, A., Cianferani, S., et al. (2020). Determination of size variants by CE-SDS for approved therapeutic antibodies: key implications of subclasses and light chain specificities. *J. Pharm. Biomed. Anal.* 184, 113166. doi:10.1016/j.jpba.2020.113166
- Wang, C., Vemulapalli, B., Cao, M., Gadre, D., Wang, J., Hunter, A., et al. (2018). A systematic approach for analysis and characterization of mispairing in bispecific antibodies with asymmetric architecture. *MAbs* 10 (8), 1226–1235. doi:10.1080/19420862.2018.1511198
- Wang, Q., Chen, Y., Park, J., Liu, X., Wang, T., McFarland, K., et al. (2019). Design and production of bispecific antibodies. *Antibodies* 8, 43. doi:10.3390/antib8030043
- Wang, A. L., Paciolla, M., Palmieri, M. J., and Hao, G. G. (2020). Comparison of glycoprotein separation reveals greater impact of carbohydrates and disulfides on electrophoretic mobility for CE-SDS versus SDS-PAGE. *J. Pharm. Biomed. Anal.* 180, 113006. doi:10.1016/j.jpba.2019.113006
- Wiesner, R., Scheller, C., Krebs, F., Wätzig, H., and Oltmann-Norden, I. (2021). A comparative study of CE-SDS, SDS-PAGE, and simple Western: influences of sample preparation on molecular weight determination of proteins. *Electrophoresis* 42 (3), 206–218. doi:10.1002/elps.202000199
- Woods, R., Xie, M., Von Kreudenstein, T., Ng, G., and Dixit, S. (2013). LC-MS characterization and purity assessment of a prototype bispecific antibody. *Mabs* 5 (5), 711–722. doi:10.4161/mabs.25488
- Wu, Y., Yi, M., Zhu, S., Wang, H., and Wu, K. (2021). Recent advances and challenges of bispecific antibodies in solid tumors. *Exp. Hematol. Oncol.* 10 (1), 56. doi:10.1186/s40164-021-00250-1
- Xu, Y., Lee, J., Tran, C., Heibeck, T., Wang, W., Yang, J., et al. (2015). Production of bispecific antibodies in “knobs-into-holes” using a cell-free expression system. *Mabs* 7 (1), 231–242. doi:10.4161/19420862.2015.989013